

Advanced Broadband Antireflection Coatings Based on Cellulose Microfiber Paper

Dongheon Ha, Joseph Murray, Zhiqiang Fang, Liangbing Hu, and Jeremy N. Munday, *Member, IEEE*

Abstract—In order to absorb a significant fraction of the incident sunlight, a solar cell must incorporate light management techniques, including high-quality antireflection coatings. Such coatings are typically produced via high-temperature deposition methods that are costly. Here, we present a new technique based on light scattering within a transparent paper that is placed on top of a solar cell. The optical and electronic responses of both Si and GaAs solar cells are tested with these coatings, and a broadband angle-insensitive response is achieved. A comparison between textured and untextured solar cells is also made, and the power conversion efficiency is improved for untextured surfaces, while the increased path length within the paper resulting from textured cells increases absorption within the paper. The process is simple and inexpensive, and the paper coatings are made from a recyclable material, leading to less environmental impact.

Index Terms—Antireflection coating (ARC), cellulose fiber, gallium arsenide, photovoltaic cells, silicon.

I. INTRODUCTION

TRADITIONAL antireflection coatings (ARCs) rely on thin-film interference effects to reduce reflection at the top interface of a solar cell. These coatings consist of either single or double layers of nonabsorbing materials with an index of refraction in between those of the surrounding material (typically air or encapsulant) and the solar cell. The thickness of the layer(s) is chosen so that the reflected light after traversing the film is 180° out of phase with the light reflected off the first surface. This way, the reflected fields cancel, and the light is transmitted into the solar cell. While these coatings are used on nearly all commercial cells, they are wavelength dependent and are deposited using expensive processes that require elevated temperatures, which increase production cost and can be detrimental to some temperature-sensitive solar cell materials.

Recently, nanostructured materials based on metal [1]–[11], dielectric [12]–[17], or semiconducting [18], [19] scatterers have been employed as alternatives to traditional ARCs. These structures typically rely on plasmonic resonances [1]–[11], whispering gallery modes [12], [13], [20]–[22], or Mie scattering [18]. While many advantages exist for these

Manuscript received July 7, 2014; revised November 24, 2014 and December 13, 2014; accepted December 29, 2014. Date of current version February 18, 2015.

D. Ha, J. Murray, and J. N. Munday are with the Department of Electrical and Computer Engineering and the Institute for Research in Electronics and Applied Physics, University of Maryland, College Park, MD 20742 USA (e-mail: dongheon@umd.edu; jmurray6@umd.edu; jnmunday@umd.edu).

Z. Fang and L. Hu are with the Department of Materials Science and Engineering, University of Maryland, College Park, MD 20742 USA (e-mail: fangzq1230@gmail.com; binghu@umd.edu).

Color versions of one or more of the figures in this paper are available online at <http://ieeexplore.ieee.org>.

Digital Object Identifier 10.1109/JPHOTOV.2015.2392940

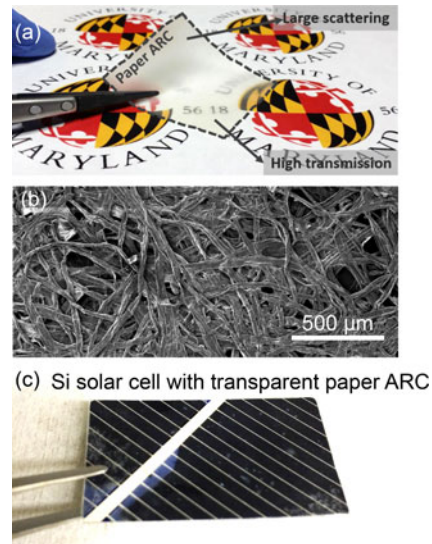


Fig. 1. Transparent paper ARC. (a) Photograph of the transparent paper showing high transmission, yet large angular scattering. (b) SEM of the cellulose fibers that make up the transparent paper. (c) Textured monocrystalline Si solar cell with transparent paper ARC attached.

subwavelength structures, their size often requires micro- and nanoscale lithography or processing.

Here, we present a new ARC that is based on microscale cellulose fibers (see Fig. 1). These fibers are constructed into a transparent paper that is able to scatter light at large angles, enabling increased optical path lengths and absorption within thin-film low-index solar cells (e.g., polymer cells). For high-index solar cells, the path length enhancement is modest but can be improved if there is sufficient scattering at the paper–semiconductor interface. We perform experiments on Si wafers, textured monocrystalline Si solar cells, and GaAs solar cells, finding that these transparent cellulose papers can act as broadband ARCs that work over a wide range of incidence angles. Additionally, these transparent paper coatings are made in a simple inexpensive process using materials that are lightweight, flexible, and recyclable.

II. TRANSPARENT CELLULOSE PAPER

Fig. 1 shows an example of the cellulose paper applied to a monocrystalline Si solar cell. The transparent paper is fabricated using TEMPO-treated micro-sized wood fibers through a papermaking technique [23], [24]. The paper has high optical transparency and also exhibits increased optical scattering [see Figs. 1(a) and 2(b)]. The high transmittance allows most of the incident light to propagate through the paper to reach the

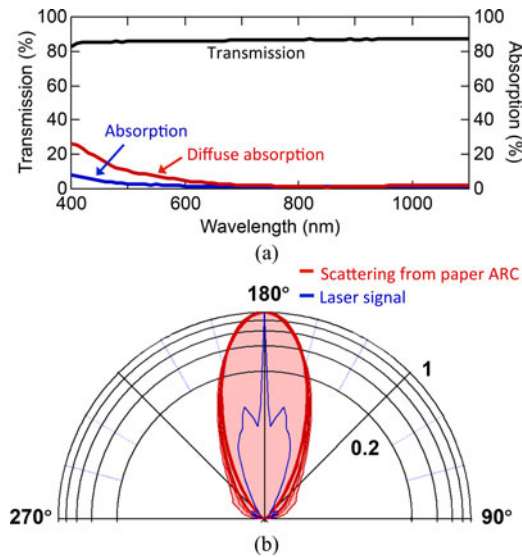


Fig. 2. Optical properties of paper coating. (a) Wavelength-dependent transmission, absorption, and diffuse absorption data show that the paper has small absorption for normally incident light; however, the absorption is increased for diffuse illumination. (b) Scattering profile under normal illumination from a tunable laser (blue) shows similar forward scattering performance (red) for all wavelengths measured (from 500 to 1000 nm).

active layer. For very thin cells, the optical scattering enables the possibility of increased path length. The normalized scattering profile of the transparent paper ARC is shown in Fig. 2(b). The paper was illuminated from normal incidence with a tunable laser with wavelengths varying from $\lambda = 500$ nm to $\lambda = 1100$ nm in 50-nm steps. The angular dependence of the transmitted signal was recorded after scattering from the paper. For comparison, the angular spread of the incident laser is shown (blue) in Fig. 2(b). There is significant scattering from the normal for all wavelengths considered, which illustrates that the paper ARC has broadband scattering properties from visible to near-infrared range.

The transmission, absorption, and diffuse absorption of the paper was measured using an integrating sphere [see Fig. 2(a)]. High transmission and low absorption are found for normal incidence illumination. However, diffuse illumination results in increased absorption, especially for shorter wavelengths. As discussed in Section IV, this increased diffuse absorption leads to decreased performance for a textured device.

The randomly oriented fibers have an average width of 20–30 μm and a length of 0.8 mm, yielding a total average film thickness of 40–50 μm . To create adhesion between the transparent paper and solar cells, a droplet of polyvinyl alcohol (PVA) is used. The capillary interaction creates a conformal coating even when a textured surface is used.

To determine the durability of the transparent paper ARC under extended solar illumination, the paper was exposed to the AM 1.5G solar spectrum for 168 h, which is equivalent to 21 days of illumination at 8 h per day. No significant degradation in the optical transmissivity (averaged across the solar spectrum) was observed (i.e., the change in transmission was found to be within the noise of the experiment $<1\%$). While future durability studies are needed, the transparent paper

appears to be a versatile and robust material for future commercial ARCs. Additionally, glass encapsulation should be considered for long-term applications, yielding further UV protection.

III. PAPER-BASED ANTIREFLECTION COATING

To determine the effect of the transparent paper ARC on the optical properties of a device, we attach the transparent paper to both a flat Si wafer and to a monocrystalline textured Si solar cell, which results in reduced reflection over all angles and wavelengths throughout the visible spectrum (see Fig. 3). The reflectivity is measured as a function of incident angle using an integrating sphere and monochromatic illumination. Fig. 3 shows contour plots of the reflectivity, which are a function of incident angle (from 10° to 55°) and wavelength (from 400 to 1000 nm). Without the transparent paper on top, the flat Si wafer generally reflects approximately 35–45% of the incident light [see Fig. 3(a), top]; however, the addition of the transparent paper ARC reduces the reflection to approximately 15–25% [see Fig. 3(a), bottom].

Because most monocrystalline Si solar cells are processed to achieve pyramidal texturing, we also consider the effect of our transparent paper on these devices. Before application of the transparent paper ARC, the device's reflectivity is reduced [see Fig. 3(b), top] in comparison with an untextured Si wafer [see Fig. 3(a), top]. The addition of the paper ARC to the textured Si solar cell further reduces the reflection [see Fig. 3(b), bottom]. Thus, the transparent paper ARC is able to reduce the reflection for both textured and untextured Si devices. This coating technique can be applied to virtually any kind of solar cell ranging from Si, which dominates the PV market, to next-generation thin-film and/or flexible solar cells.

The transparent paper ARC also shows little dependence on the incident angle of illumination, which reduces the need for a mechanical tracking system to align the surface normal of the solar cell with the incident light from the sun (see Fig. 3). We attribute the reduced angular dependence to the surface texturing of the transparent paper ARC, which helps light enter this ARC even at steep angles.

An incoherent optical reflection model can be used to explain the reduction of the reflectivity upon application of the transparent paper ARC. We used this incoherent light propagation model rather than a coherent one because the ARC is relatively thick ($\sim 50 \mu\text{m}$) and slightly textured. Thus, the phase accumulated as the light propagates through the film is not spatially uniform as it would be for a thin flat film. The Fresnel equations based on the incoherent light propagation are used to model the reflection from the Si wafer with and without the transparent paper ARC. The two components for each polarization are

$$R_S = \left| \frac{n_1 \cos \theta_i - n_2 \cos \theta_t}{n_1 \cos \theta_i + n_2 \cos \theta_t} \right|^2 \quad (1)$$

and

$$R_P = \left| \frac{n_1 \cos \theta_t - n_2 \cos \theta_i}{n_1 \cos \theta_t + n_2 \cos \theta_i} \right|^2 \quad (2)$$

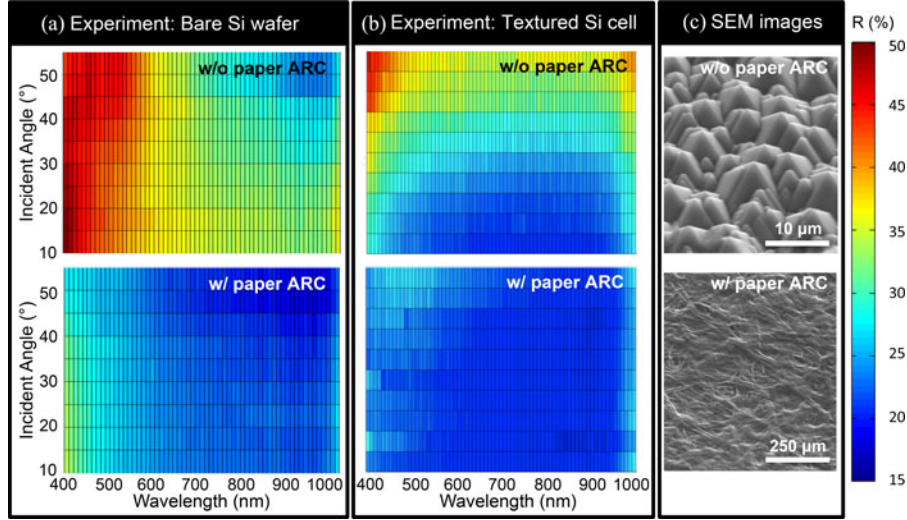


Fig. 3. Transparent paper ARC reduces reflection over a wide range of incident angles and wavelengths. (a) Measurements of the reflectivity of a bare Si wafer (top) and the same wafer after the application of the transparent paper ARC (bottom) as a function of incident angle (from 10° to 55°) and wavelength (from 400 to 1000 nm). Contour plots show that the reflectivity is reduced for all wavelengths and incident angles. (b) Measurements of the reflectivity for a textured monocrystalline Si solar cell without (top) and with (bottom) the transparent paper ARC. Similarly, the reflection is reduced for all wavelengths and incident angles. (c) SEM of the top surface of the textured monocrystalline Si solar cell with pyramidal structuring on the surface (top). After attachment of the transparent paper ARC, the pyramidal structures are no longer visible and only the larger scale cellulose fibers can be seen (bottom).

where n_1 and n_2 are the refractive indexes of the two media at the interface, and θ_i and θ_t are the incident and transmitted angles from the surface normal, respectively.

As the light reaches each surface, a fraction is reflected and the remainder is transmitted, as determined by the Fresnel equations. This process leads to an infinite sum, which is schematically shown in Fig. 4(a). To calculate the total reflectivity at the air interface, we consider a geometric sequence, resulting in the total reflectivity:

$$R_{\text{TOTAL}} = R_{\text{ARCtoAIR}} + \frac{T_{\text{AIRtoARC}} \cdot R_{\text{WAFERtoARC}} \cdot T_{\text{ARCtoAIR}}}{1 - R_{\text{WAFERtoARC}} \cdot R_{\text{AIRtoARC}}} \quad (3)$$

where R and T represent the reflectivity and transmissivity, respectively, at the interface described by their subscript.

As shown in Fig. 4, the calculated reflectivity based on this model both with [see Fig. 4(c)] and without [see Fig. 4(b)] the transparent paper ARC agrees well with the experimental data [see Fig. 3(a)] for nearly all wavelengths and incident angles. The refractive index of the ARC is taken to be $n = 1.47$, which is the refractive index of the cellulose fibers making up the paper [25] and also the PVA for attachment [26]. However, for the largest angles, the model appears to overestimate the reflectivity when the paper ARC is used. We attribute this result to the texture of the paper, which reduces the angular dependence.

In the next section, we will consider the electrical performance of a textured monocrystalline Si solar cell and compare it with a planar GaAs solar cell, both with and without the transparent paper ARC.

IV. OPTOELECTRONIC RESPONSE OF COATED SOLAR CELLS

In order to determine the effect of the transparent paper on a fully processed solar cell, the paper is transferred to two different

types of devices: an untextured GaAs solar cell (M-Comm) and a textured monocrystalline Si solar cell (SensLite). Both devices show a significant decrease in the optical reflectivity. The flat untextured GaAs cell also shows a significant increase in the photocurrent as a result of the coating; however, the textured monocrystalline Si device shows a decrease in the photocurrent. This decrease is suspected to arise as a result of small amounts of absorption in the paper-based ARC, which are increased by the enhanced path length within the paper due to scattering from the textured pyramidal surface of the monocrystalline Si solar cell as described at the end of this section.

The GaAs solar cell's efficiency (η) was determined under AM 1.5G illumination using a solar simulator. Fig. 5(a) shows the measured current density–voltage (J - V) characteristics of the cell. The cell's electronic properties are extracted from the J - V curve. With the transparent paper ARC on top of the same GaAs cell, the total power conversion efficiency is improved by 23.9%, from $\eta = 13.6\%$ to $\eta = 16.8\%$. The improvement is predominantly due to an increase in the short-circuit current density, J_{SC} , (20.5%). A modest improvement in the fill factor (FF) (2.6%) is also obtained; however, there is almost no change in the open-circuit voltage V_{OC} . The external quantum efficiency (EQE) of the GaAs solar cell was also determined and is shown in the inset of Fig. 5(a). By attaching the transparent paper ARC, the EQE of the GaAs solar cell is improved throughout the entire wavelength range (from 400 to 900 nm). The electronic properties of GaAs solar cell with and without the transparent paper ARC are summarized in Table I.

The monocrystalline Si solar cell's efficiency was also determined under AM 1.5G illumination; however, despite the decreased reflectivity, the photocurrent was not enhanced. To understand this surprising result, the optical properties of the paper and the scattering at the Si interface must be carefully considered. While the paper has high transmission, we found that it

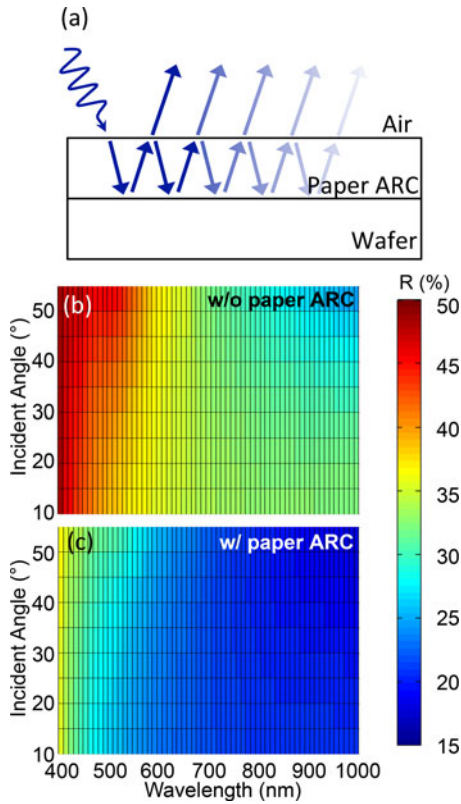


Fig. 4. Incoherent light propagation model explains well the measured reflectivity. (a) Schematic of light propagation and reflection with the transparent paper ARC. Angular and wavelength dependence of reflection from a Si wafer with (c) and without (b) the paper-based ARC. Results of the model are in close agreement with the experimental values [see Fig. 3(a)].

also absorbs approximately 2.1% of the incident light (averaged across the solar spectrum) when placed on a glass slide and measured using an integrating sphere. When the paper is placed on a flat surface, the path length is only enhanced slightly due to the texturing of the paper itself. However, when placed on top of the textured Si, the paper leads to increased wide angle backing scattering of the light as it is reflected off the Si surface. The increased path length within the paper can result in nonnegligible absorption within the layer. This effect is clearly observable in the diffuse absorption measurement [see Fig. 2(a)], which shows increased absorption within the paper for light entering at nonnormal incidence angles. The reflectivity is still reduced upon the addition of the paper ARC; however, a larger fraction of the absorption occurs in the paper when the Si layer is textured, leading to a decrease in the measured photocurrent. The electronic properties for both the bare monocrystalline Si solar cell and the cell with the paper ARC are shown in Table II.

In order to recover the advantageous antireflection properties of the paper when applied to a textured device, the absorption within the paper needs to be decreased. This can be achieved either by development of papers with less absorption or with papers that are thinner, which would decrease the optical path length. In order to calculate the expected performance improvement with such a paper ARC, we calculate the expected short-circuit current density increase upon application of the paper ARC based on the experimentally determined decrease

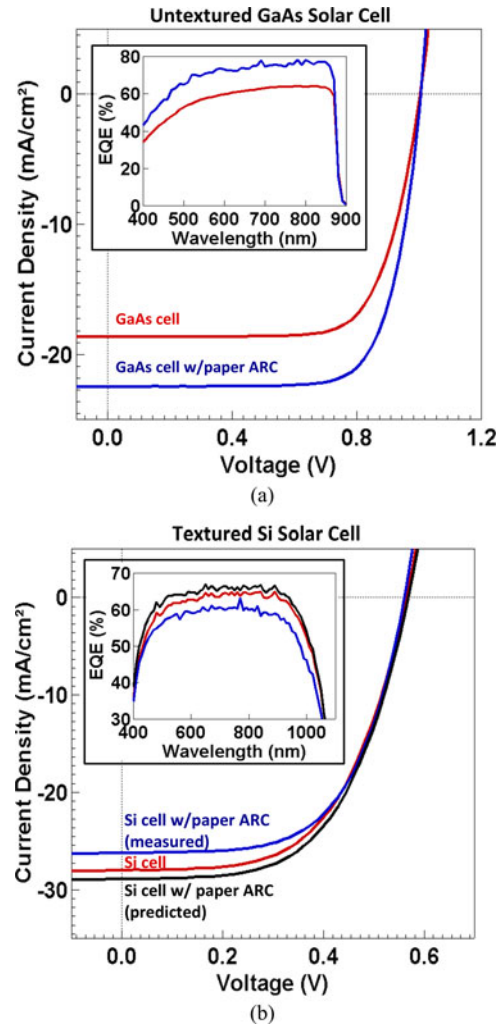


Fig. 5. J - V characteristics for textured (Si) and untextured (GaAs) solar cells both with and without the transparent paper ARCs. (a) Addition of the transparent paper ARC to a GaAs solar cell resulted in a J_{SC} of 22.49 mA/cm^2 , which is approximately 20.5% higher than that from the cell without the ARC. Due to a slight increase in FF as well as the large enhancement in J_{SC} , there is a 23.9% increase in the power conversion efficiency. (b) For the textured monocrystalline Si solar cell, adding the transparent paper ARC reduced the cell's J_{SC} and the power conversion efficiency as a result of increased light absorption within the transparent paper ARC layer. For a thinner or less absorbing paper, the J_{SC} could be increased to 28.91 mA/cm^2 (compared with 28.02 mA/cm^2 for the device without ARC) as determined from the decrease in the measured reflectivity. We predict that the efficiency would reach 9.39%, an improvement of 3.8%.

TABLE I
COMPARISON OF ELECTRONIC PROPERTIES BETWEEN THE BARE GAAS CELL AND THE CELL WITH TRANSPARENT PAPER ARC

	V_{OC} (mV)	J_{SC} (mA/cm^2)	FF (%)	Efficiency (%)
Bare GaAs cell	1001.9 ± 0.3	18.67 ± 0.01	72.5 ± 0.5	13.55 ± 0.10
With ARC	1004.0 ± 0.5	22.49 ± 0.01	74.4 ± 0.2	16.79 ± 0.03
Enhancement	0.21%	20.46%	2.62%	23.91%

in the reflectivity [see Fig. 3(b)]. Under AM 1.5G illumination, J_{SC} would be increased by 0.89 mA/cm^2 , corresponding to a 3.2% increase in the J_{SC} over the bare cell. Fig. 5(b) shows the J - V characteristic for the textured Si solar cell without paper ARC, with paper ARC, and the expected J - V characteristic

TABLE II
COMPARISON OF ELECTRONIC PROPERTIES BETWEEN THE BARE SI CELL AND THE CELL WITH TRANSPARENT PAPER ARC

	V_{OC} (mV)	J_{SC} (mA/cm ²)	FF (%)	Efficiency (%)
Bare Si cell	563.9 ± 0.3	28.02 ± 0.02	57.3 ± 1.0	9.05 ± 0.20
With ARC	559.8 ± 0.1	26.25 ± 0.01	60.5 ± 0.1	8.90 ± 0.01
Lossless ARC (Predicted)	568.1 ± 0.3	28.91 ± 0.02	57.2 ± 1.0	9.39 ± 0.20

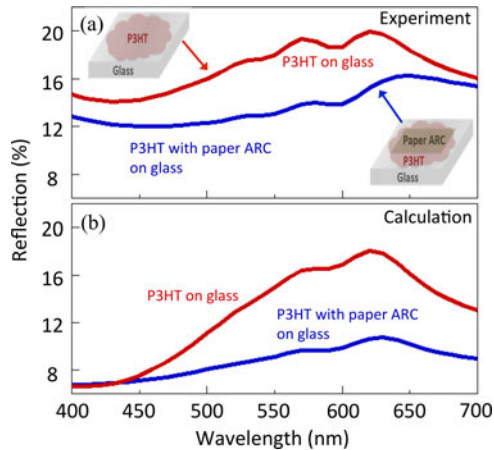


Fig. 6. Reflectivity of a polymer (P3HT) on glass is reduced upon the addition of a paper ARC, showing potential application for thin film organic photovoltaic devices. Experimental results (a) are in reasonable agreement with predictions (b) based on a transfer matrix method (neglecting scattering).

if there were no loss in the paper. The expected J - V curve is obtained by adding 0.89 mA/cm² to the photogenerated current measured from the device without the paper ARC. In the same way, we can estimate the expected EQE of the device with the addition of a lossless transparent paper ARC on the textured Si solar cell. As shown in the inset of Fig. 5(b), the lossless transparent paper ARC applied to the textured Si solar cell would also improve EQE throughout the entire wavelength range for the solar cell (from 400 to 1100 nm). However, the enhancement is not remarkable compared with the GaAs solar cell because the textured bare Si solar cell already has good optical absorptivity at near normal incidence as shown in Fig. 3(b). Thus, adding this transparent paper ARC is not able to bring as large of an enhancement in EQE, when compared with the untextured cell at normal incidence.

Due to the difference in the refractive index between the paper ARC and the GaAs or Si substrate, it is difficult to reduce reflection below $\sim 15\%$ without grading the index or increasing the scattering at the interface. For a lower index substrate (e.g., P3HT, a common polymer solar cell material), the paper ARC can have improved performance due to a more optimal index contrast. To further investigate this idea, we performed reflection measurements on P3HT with and without the paper ARC (see Fig. 6). To prepare the sample, a droplet of the P3HT solution was spun onto glass, and a thickness of ~ 60 nm was achieved, as determined by ellipsometry. This paper ARC effec-

tively reduces light reflection throughout the entire wavelength range of interest for this polymer (from 400 to 700 nm). In this range, the solar spectrum-weighted light reflection was reduced from 17.0% to 13.7% with the addition of the paper ARC, corresponding to an $\sim 20\%$ overall reduction. To determine how much the reduced reflection depends on the index contrast alone, the reflection was calculated under the simplifying assumption of no scattering using the well-known matrix transfer method [27] where the P3HT was treated as a coherent layer and the paper and glass were treated as incoherent layers. The glass was assumed to have an index of 1.5, the paper, an index of 1.47, and the P3HT, an index derived from [28]. Despite the small discrepancy in the magnitude between the experiment and calculation, it is clear that the paper ARC can perform well even on a lower index substrate. The difference between the experiment and calculation is likely due to the difference between the refractive indices of the P3HT layer in the calculations and the experiments and due to scattering by the paper, which is not included in the calculation. For shorter wavelengths (from 400 to 450 nm), the effect of the paper ARC is not significant in the calculation. In this wavelengths range, the refractive index of P3HT is slightly lower than the paper ARC, and thus, the gradual index contrast from air to the polymer is not obtained. For this reason, light reflection becomes slightly larger. By contrast, the decreased reflection measured experimentally in this range is likely due to light scattering within the paper ARC.

While additional improvement is needed for these paper-based coatings to surpass the normal incidence performance of interference-based coatings, there are many advantages to the cellulose paper ARCs. From a manufacturing point of view, this room temperature fabrication process has the potential to reduce manufacturing costs. From an optical point of view, the angular independence of the paper-based ARC gives additional competitiveness to this technique, as it reduces the need for solar tracking. As a roadmap to ultralow reflectivity, future designs could consist of multiple paper layers with different packing densities to create graded index ARCs that could match or exceed the performance of traditional double-layer interference coatings.

V. CONCLUSION

In conclusion, we have observed improved optical response from solar cells using a novel transparent paper-based antireflection coating. The paper leads to a significant decrease in the reflectivity independent of incident illumination angle for both textured and untextured cells. An increase in the power conversion efficiency for the untextured cells is also observed; however, cells with surface texturing have reduced power conversion efficiencies due to an increase in the absorption within the paper ARC resulting from an increased path length within the coating. This study also shows the need for testing beyond simple reflection measurements to determine the effects of potential ARCs. Despite drawbacks on devices with textured surfaces, this new type of ARC offers a simple, earth abundant material option and a room-temperature deposition process, making this technique an excellent candidate for planar solar cell technologies.

Additionally, thinner transparent papers could provide superior performance for textured devices by further reducing the loss within the paper.

REFERENCES

- [1] V. E. Ferry, J. N. Munday, and H. A. Atwater, "Design considerations for plasmonic photovoltaics," *Adv. Mater.*, vol. 22, pp. 4794–4808, 2010.
- [2] H. R. Stuart and D. G. Hall, "Island size effects in nanoparticle-enhanced photodetectors," *Appl. Phys. Lett.*, vol. 73, pp. 3815–3817, 1998.
- [3] J. N. Munday and H. A. Atwater, "Large integrated absorption enhancement in plasmonic solar cells by combining metallic gratings and antireflection coatings," *Nano Lett.*, vol. 11, pp. 2195–2201, 2010.
- [4] H. A. Atwater and A. Polman, "Plasmonics for improved photovoltaic devices," *Nature Mater.*, vol. 9, pp. 205–213, 2010.
- [5] K. R. Catchpole and A. Polman, "Design principles for particle plasmon enhanced solar cells," *Appl. Phys. Lett.*, vol. 93, pp. 19113-1–19113-3, 2008.
- [6] K. R. Catchpole and A. Polman, "Plasmonic solar cells," *Opt. Exp.*, vol. 16, no. 26, pp. 21793–21800, 2008.
- [7] Q. Gan, F. J. Bartoli, and Z. H. Kafafi, "Plasmonic-enhanced organic photovoltaics: Breaking the 10% efficiency barrier," *Adv. Mater.*, vol. 25, pp. 2385–2396, 2013.
- [8] I. K. Ding, J. Zhu, W. Cai, S.-J. Moon, N. Cai, P. Wang, S. M. Zakeeruddin, M. Grätzel, M. L. Brongersma, Y. Cui, and M. D. McGehee, "Plasmonic dye-sensitized solar cells," *Adv. Energy Mater.*, vol. 1, pp. 52–57, 2011.
- [9] J. Bhattacharya, N. Chakravarty, S. Pattnaik, W. Dennis Slafer, R. Biswas, V. L. Dalal, "A photonic-plasmonic structure for enhancing light absorption in thin film solar cells," *Appl. Phys. Lett.*, vol. 99, pp. 13114-1–13114-3, 2011.
- [10] R. A. Pala, J. White, E. Barnard, J. Liu, and M. L. Brongersma, "Design of plasmonic thin-film solar cells with broadband absorption enhancements," *Adv. Mater.*, vol. 21, pp. 3504–3509, 2009.
- [11] C. Hägglund, M. Zäch, G. Petersson, and B. Kasemo, "Electromagnetic coupling of light into a silicon solar cell by nanodisk plasmons," *Appl. Phys. Lett.*, vol. 92, pp. 053110-1–053110-3, 2008.
- [12] J. Grandidier, D. M. Callahan, J. N. Munday, and H. A. Atwater, "Thin-film solar cells: Light absorption enhancement in thin-film solar cells using whispering gallery modes in dielectric nanospheres," *Adv. Mater.*, vol. 23, pp. 1171–1171, 2011.
- [13] J. Grandidier, D. M. Callahan, J. N. Munday, and H. A. Atwater, "Gallium arsenide solar cell absorption enhancement using whispering gallery modes of dielectric nanospheres," *IEEE J. Photovoltaics*, vol. 2, no. 2, pp. 123–128, Apr. 2012.
- [14] J. Grandidier, R. A. Weitekamp, M. G. Deceglie, D. M. Callahan, C. Battaglia, C. R. Bukowsky, C. Ballif, R. H. Grubbs, and H. A. Atwater, *Phys. Status Solidi (a)*, vol. 210, pp. 255–260, 2013.
- [15] D. Derkacs, W. V. Chen, P. M. Matheu, S. H. Lim, P. K. L. Yu, and E. T. Yu, "Nanoparticle-induced light scattering for improved performance of quantum-well solar cells," *Appl. Phys. Lett.*, vol. 93, pp. 091107-1–091107-3, 2008.
- [16] J. Zhu, C.-M. Hsu, Z. Yu, S. Fan, and Y. Cui, "Nanodome solar cells with efficient light management and self-cleaning," *Nano Lett.*, vol. 10, pp. 1979–1984, 2010.
- [17] M. Kroll, S. Fahr, C. Helgert, C. Rockstuhl, F. Lederer, and T. Pertsch, "Employing dielectric diffractive structures in solar cells—A numerical study," *Phys. Status Solidi (a)*, vol. 205, pp. 2777–2795, 2008.
- [18] P. Spinelli, M. A. Verschuuren, and A. Polman, "Broadband omnidirectional antireflection coating based on subwavelength surface Mie resonators," *Nature Commun.*, vol. 3, pp. 692-1–692-5, 2012.
- [19] M. L. Brongersma, Y. Cui, and S. Fan, "Light management for photovoltaics using high-index nanostructures," *Nature Mater.*, vol. 13, pp. 451–560, 2014.
- [20] J. Yin, Y. Zang, C. Yue, X. He, a. Jing Li, Z. Wu, and Y. Fang, "Self-assembled hollow nanosphere arrays used as low Q whispering gallery mode resonators on thin film solar cells for light trapping," *Phys. Chem. Chem. Phys.*, vol. 15, pp. 16874–16882, 2013.
- [21] M. Mariano, F. J. Rodríguez, P. Romero-Gomez, G. Kozyreff, and J. Martorell, "Light coupling into the whispering gallery modes of a fiber array thin film solar cell for fixed partial Sun tracking," *Sci. Rep.*, vol. 4, pp. 4959-1–4959-6, 2014.
- [22] Y. Yao, J. Yao, V. K. Narasimhan, Z. Ruan, C. Xie, S. Fan, and Y. Cui, "Broadband light management using low-Q whispering gallery modes in spherical nanoshells," *Nature Commun.*, vol. 3, pp. 664-1–664-7, 2012.
- [23] Z. Fang, H. Zhu, Y. Yuan, D. Ha, S. Zhu, C. Preston, Q. Chen, Y. Li, X. Han, S. Lee, G. Chen, T. Li, J. Munday, J. Huang, and L. Hu, "Novel nanostructured paper with ultrahigh transparency and ultrahigh haze for solar cells," *Nano Lett.*, vol. 14, pp. 765–773, 2014.
- [24] D. Ha, Z. Fang, L. Hu, and J. N. Munday, "Paper-based anti-reflection coatings for photovoltaics," *Adv. Energy Mater.*, vol. 4, pp. 1301804-1–1301804-5, 2014.
- [25] S. N. Kasarova, N. G. Sultanova, C. D. Ivanov, and I. D. Nikolov, "Analysis of the dispersion of optical plastic materials," *Opt. Mater.*, vol. 29, pp. 1481–1490, 2007.
- [26] S. Hayashi, K. Asada, S. Horiike, H. Furuhashi, and T. Hirai, "Piezochromism of porous poly(vinyl alcohol)-poly(vinyl acetate) composite film in organic solvents," *J. Colloid Interface Sci.*, vol. 176, pp. 370–377, 1995.
- [27] C. C. Katsidis and D. I. Siapkas, "General transfer-matrix method for optical multilayer systems with coherent, partially coherent, and incoherent interference," *Appl. Opt.*, vol. 41, pp. 3978–3987, 2002.
- [28] *CompleteEASE, Ver. 4.72 (Computer Program)*, J.A. Woollam Co. Inc., Lincoln, NE, USA, 2012.



Dongheon Ha received the B.S. degree in computer science and electrical engineering (with honors) from Handong University, Pohang, Korea, and the M.S. degree in electrical engineering from the Korea Advanced Institute of Science and Technology, Daejeon, Korea. He is currently working toward the Ph.D. degree with Prof. J. N. Munday and his colleagues at the University of Maryland, College Park, MD, USA.

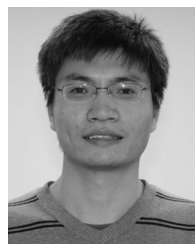
His research interests include design and analysis of dielectric antireflection coatings for future solar cells.



Joseph Murray received the B.S. degree in physics and the Masters of Science degree in electrical engineering, with a thesis on laser texturing of SiC photodetectors, both from the University of Virginia, Charlottesville, VA, USA, in 2006 and 2010, respectively. He is currently working toward the Ph.D. degree with the University of Maryland, College Park, MD, USA, working with Prof. J. N. Munday in the Department of Electrical and Computer Engineering.

His research interests include solar cell physics and the fundamental limits on absorption and effi-

ciency.



Zhiqiang Fang is currently working toward the Ph.D. degree with the State Key Laboratory of Pulp and Paper Engineering, South China University of Technology, Guangzhou, China.

He is also currently a Visiting Student with the Materials Science and Engineering Department, University of Maryland, College Park, MD, USA, under the supervision of Prof. L. Hu. His current research interests include nanomaterials and nanostructures, paper-based flexible electronics, and energy storage devices.



Liangbing Hu received the B.S. degree in applied physics from the University of Science and Technology of China (USTC) in 2002 and the Ph.D. degree from The University of California at Los Angeles, Los Angeles, CA, USA, focusing on carbon nanotube-based nanoelectronics.

In 2006, he joined Unidym, Inc., as a Cofounding Scientist. At Unidym, his role was the development of roll-to-roll printed carbon nanotube transparent electrodes and device integrations into touch screens, LCDs, flexible OLEDs, and solar cells. He was with Stanford University, Stanford, CA, USA, from 2009 to 2011, where he worked on various energy devices based on nanomaterials and nanostructures. He is currently an Assistant Professor with the University of Maryland College Park, MD, USA. His research interests include nanomaterials and nanostructures, roll-to-roll nanomanufacturing, energy storage and conversion, and printed electronics.



Jeremy N. Munday (M'06) received the B.S. degree in physics from Middle Tennessee State University, Murfreesboro, TN, USA, in 2003, and the M.A. and Ph.D. degrees in physics from Harvard University, Cambridge, MA, USA, in 2005 and 2008, respectively. He is currently an Assistant Professor with the Department of Electrical and Computer Engineering and the Institute for Research in Electronics and Applied Physics, University of Maryland, College Park, MD, USA. Prior to this, he was a Postdoctoral Research Scholar with the California Institute of Technology, Pasadena, CA, USA.

His research interests include next-generation photovoltaics, alternative energy, engineering acoustic and electromagnetic materials, plasmonics, and quantum electrodynamic phenomena, such as the Casimir effect. His research has been published in a variety of international journals, and he has contributed chapters to three books. Dr. Munday is a Member of the American Physical Society, Sigma Pi Sigma, the Materials Research Society, the International Society for Optics and Photonics, and the Optical Society of America. He received the SPIE Early Career Achievement Award, the IEEE Photonics Society Young Investigator Award, and the NASA Early Career Faculty Space Technology Research Award.